11-*cis*-Retinal Protonated Schiff Base: Influence of the Protein Environment on the Geometry of the Rhodopsin Chromophore†

Minoru Sugihara,*,‡ Volker Buss,*,§ Peter Entel,‡ Marcus Elstner,|| and Thomas Frauenheim||

Institute of Theoretical Low-Temperature Physics, University of Duisburg, D47048 Duisburg, Germany, Institute of Physical and Theoretical Chemistry, University of Duisburg, D47048 Duisburg, Germany, and Institute of Theoretical Physics, University of Paderborn, D33098 Paderborn, Germany

Received August 15, 2002

ABSTRACT: Density functional theory (DFT) calculations based on the self-consistent-charge tight-binding approximation have been performed to study the influence of the protein pocket on the 3-dimensional structure of the 11-*cis*-retinal Schiff base (SB) chromophore. Starting with an effectively planar chromophore embedded in a protein pocket consisting of the 27 next-nearest amino acids, the relaxed chromophore geometry resulting from energy optimization and molecular dynamics (MD) simulations has yielded novel insights with respect to the following questions: (i) The conformation of the β-ionone ring. The protein pocket tolerates both conformations, 6-s-cis and 6-s-trans, with a total energy difference of 0.7 kcal/mol in favor of the former. Of the two possible 6-s-cis conformations, the one with a negative twist angle (optimized value: −35°) is strongly favored, by 3.6 kcal/mol, relative to the one in which the dihedral is positive. (ii) Out-of-plane twist of the chromophore. The environment induces a nonplanar helical deformation of the chromophore, with the distortions concentrated in the central region of the chromophore, from C10 to C13. The dihedral angle between the planes formed by the bonds from C7 to C10 and from C13 to C15 is 42°. (iii) The absolute configuration of the chromophore. The dihedral angle about the C12−C13 bond is +170° from planar s-cis, which imparts a positive helicity on the chromophore, in agreement with earlier considerations based on theoretical and spectroscopic evidence.

11-*cis*-Retinal is the chromophore of rhodopsin, the photoreceptor which is responsible for light/dark vision in the vertebrate eye. Linked covalently as a protonated Schiff base (pSB)[1] to the ϵ-amino group of Lys296 (*1*), the chromophore is activated by light and initiates in response a sequence of events which eventually leads to excitation of the visual nerve and the perception of light in the brain. Elucidating the mechanism which governs this extremely intricate process has been a challenge ever since the seminal studies, more than 30 years ago, by Wald (*2*, *3*), who was able to show that the triggering event of vision is the photochemical isomerization of 11-*cis*-retinal to the all-trans form. This first intermediate, bathorhodopsin, is formed within 200 fs in an extremely fast and efficient reaction (*4*, *5*). In the subsequent events, the local configurational change of the chromophore is translated, via several spectroscopically identified intermediates (*6*−*10*), into conformational changes of the whole protein. Eventually the strongly blue-shifted metarhodopsin II is reached in which the salt-bridge between the SB and the protein is broken and large-scale helical motions are observed (*11*, *12*). Meta II, the so-called signaling state, acts as a template for the heterotrimeric G-protein transducin which starts the strongly amplificating G-protein or visual cascade and effects the closing of millions of membrane cation channels (*13*).

Recently the X-ray crystal structure analysis of bovine rhodopsin has been reported at 2.8 Å resolution (*14*, *15*). This study is considered a milestone since it presents the first high-resolution structure of a member of the super family of G-protein coupled receptor proteins. Rhodopsin molecules are packed in the crystal lattice to form an array of helical tubes, with each of the asymmetric units containing two rhodopsin molecules, A and B, respectively. The diffraction data clearly show the seven membrane spanning helices as well as the extracellular and the cytoplasmatic domains; about 93% of the amino acid side chains are resolved. The chromophore is represented by a well-defined density profile, and its conformation appears to be 6-s-cis,11-cis,12-s-trans,15-16-anti. The chromophore is assumed to be protonated, though this fact is not discernible from the X-ray data.

† This work was supported by the Graduated School on Structure and Dynamics of Heterogeneous Systems at the University of Duisburg and the Research Group Molecular Mechanisms of Retinal Protein Action by the German Research Council.

* Corresponding authors. M.S.: tel (+49) 203-379-2794, fax (+49) 203-379-3665, e-mail minoru@thp.uni-duisburg.de. V.B.: tel (+49) 203-379-3315, fax (+49) 203-379-2772, e-mail theobuss@uni-duisburg.de.

‡ Institute of Theoretical Low-Temperature Physics, University of Duisburg.

§ Institute of Chemistry, University of Duisburg.

|| Institute of Theoretical Physics, University of Paderborn.

[1] Abbreviations: CASPT2, multiconfigurational second-order perturbation theory; CD, circular dichroism; CG, conjugate gradient; CI, configuration iteration; DFT, density functional theory; HF, Hartree−Fock; MNDO, modified neglect of diatomic overlap; MD, molecular dynamics; NMR, nuclear magnetic resonance; pSB, protonated Schiff base; SB, Schiff base; SCC-DFTB, self-consistent-charge density functional based tight binding; UV−vis, ultraviolet−visible.

10.1021/bi020533f CCC: $22.00
Published on Web 11/28/2002

Glu113 serves as a counterion to the positive charge of the chromophore (*16*, *17*). The two oxygens of the carboxylate side chain are located 3.3 and 3.5 Å, respectively, from the pSB nitrogen. Glu113 and Lys296, to which the chromophore is covalently bound, are two of the key amino acid residues that define the position of the rhodopsin chromophore. In all, 27 amino acid residues have been identified within 4.5 Å of the retinal moiety.

The X-ray structure of rhodopsin presents a major step toward understanding the mechanistic details of the visual process. Using the experimental geometry of the protein as a point of departure, possible pathways and structures of intermediates may be envisaged and tested using theoretical methods. However, major uncertainties regarding the ground-state structure of the chromophore remain which have not been answered and which may be crucial for modeling its later stages:

- What is the conformation of the β-ionone ring relative to the chromophore? Though it has been long assumed that the geometry is twisted 6-s-cis (*18*), a recent NMR (nuclear magnetic resonance) spectroscopic study has cast doubts on this and proposed that the conformation is derived from 6-s-trans instead (*19*). The diffraction data do not allow an unambiguous assignment. Since movement of the β-ionone terminus may be a crucial step for the activation of the protein (*20*), this question needs clarification.
- What is the conformation of the chromophore chain? There are indications that the chromophore is strongly twisted in the central region, from C10 to C13 (*21*−*24*). This twist may be responsible for the initial ultrafast isomerization reaction since it induces a significant slope with respect to C11−C12 torsion in the Franck−Condon region of the excited-state potential energy surface (*25*−*27*). The resolution of the diffraction data is not sufficient for determining out-of-plane torsional angles and cannot render a reliable 3-dimensional structure of the chromophore on which to base high-quality excited-state calculations.
- What is the absolute conformation of the retinal chromophore inside the protein pocket? Nonplanar mirror-image conformations of the chromophore behave differently in the asymmetric environment of the protein. With the high efficiency and selectivity of the photoreaction and probably the subsequent reactions as well, it appears inconceivable that the reaction pathways starting from mirror-image conformations have the same probability. Also, the correct chromophore conformation is necessary for obtaining a correct model of the rhodopsin reaction center. Studying the extent of chiral discrimination is a major step toward understanding the interaction between the chromophore and the protein.

With questions such as these in mind we have analyzed the influence of the protein environment on the geometry of the rhodopsin chromophore. We have employed for this study a recently developed theoretical method which is based on DFT and which allows the inclusion of a large portion of the protein. In the next section, we will describe the method and the molecular model on which the calculations are based. We will then present the results in the order of the questions raised and discuss their relevance with respect to what is presently known about the chromophore geometry of rhodopsin.

METHOD AND MODEL

Method. All calculations were performed using the self-consistent-charge density functional based tight-binding (SCC-DFTB) method (*28*). This method is based on a second-order expansion of the Kohn−Sham total energy with respect to charge density fluctuations. The zero-order approach is equivalent to a common standard nonself-consistent scheme, while at second order a transparent, parameter-free, and readily calculable expression for generalized Hamiltonian matrix elements is derived. The method has been applied with success to the study of solid-state materials and semiconductor surfaces, but also to organic molecules and biological systems (*29*−*31*). For geometry optimization we have employed the conjugated gradient (CG) method, and for MD calculations the system was described as a micro-canonical ensemble. Only the SCC-DFTB code was used in all calculation including the MD simulations.

Model. The calculations are based on the coordinates of bovine rhodopsin deposited as 1F88 in the Protein Data Bank (*14*). Of the two rhodopsin molecules making up the asymmetric unit, molecule A was chosen as the basis of our model. It considers the chromophore plus the 27 amino acid residues which are within 4.5 Å distance from the retinal molecule and form the immediate environment, or the protein pocket, of the chromophore. These amino acids have been identified by Palczewski (*14*) and consist of Tyr43, Met44, Leu47, Thr94, Glu113, Ala117, Thr118, Gly120, Gly121, Glu122, Tyr178, Glu181, Ser186, Cys187, Gly188, Ile189, Tyr191, Met207, His211, Phe212, Phe261, Trp265, Tyr268, Ala269, Phe293, Ala295, and Lys296. For the model, the complete amino acids were considered including their part of the peptide backbone, the $-N-C_\alpha-C-$ moieties. Where the backbone was interrupted, the valencies of the exposed C and N atoms were saturated by the necessary number of hydrogen atoms. During the simulations, only the backbone atoms were kept fixed in space.

The retinal binding site contains three glutamic acids. One is Glu113, the negative counterion of the chromophore (*16*, *17*) which provides the salt bridge with the protonated chromophore; the other two are Glu122 and Glu181. In the Fourier transform infrared difference spectra of the mutant E122Q, the carboxyl group of Glu122 shows C═O stretching bands in the dark state indicating that the group is protonated (*32*). Also, according to recent results of UV−vis (ultraviolet−visible) spectroscopy of site-directed mutants, Glu181 is protonated in the ground state of rhodopsin and does not serve a counterion function (*33*). Thus, our model of the retinal binding site of rhodopsin is neutral in accordance with the results of two-photon spectroscopy (*34*). There are no water molecules near the retinal binding site in the crystal structure. However, there are several cavities within the rhodopsin molecule of sufficient size to hold one or more water molecules. Two of these cavities are near the chromophore. One of them is close to Glu113, and the other one is on the opposite side of the SB nitrogen atom away from Glu113 (*15*). Fourier transform infrared spectroscopy shows that one or a few water molecules are located in the proximity of Glu113, the counterion of the SB (*35*, *36*). Accordingly, we have inserted one water molecule into the cavity close to Glu113. Calculations were started with the initial chromophore geometry from 1F88 except for the dihedral angles

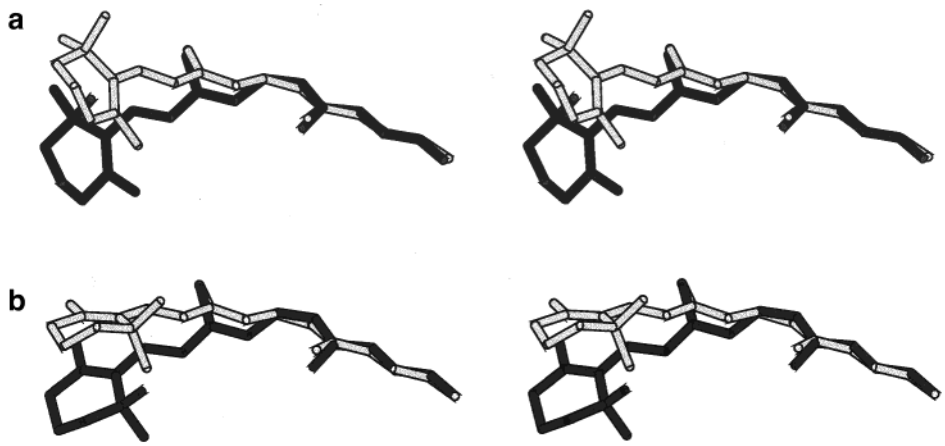

FIGURE 1: Stereoview (cross-eyed) of the minimized conformations of the retinal chromophore in the protein pocket (black) against the isolated planar conformation (white). (a) 6-s-*cis*-11-*cis*-retinal pSB. (b) 6-s-*trans*-11-*cis*-retinal pSB.

which were set to planar-trans or planar-cis from C7 to the SB nitrogen. The other structural parameters (bond lengths and angles) were adopted from the crystal structure.

RESULTS

As a point of reference, we have calculated the geometry of the 11-*cis*-retinal pSb in the isolated state without the protein environment. Except for the C6−C7 bond, the chromophore is almost planar, the largest deviation occurring for the C8−C9 single bond with a torsion angle of 5° from planar trans. In particular, the central part of the chromophore, from C10 to C13, is not twisted, as might be anticipated from the steric interaction between the C13 methyl group and the C10 hydrogen. Instead of bond torsion, this interaction is relieved by in-plane bending of the methyl group: the C12−C13−C20 bond angle is widened, from 119.9° in all-*trans*-retinal pSb to 122.4° in the 11-cis isomer. Obviously, the gain in delocalization energy of the charged chromophore is sufficient to offset the bond angle strain. With respect to torsion around the C5−C6−C7−C8, three different conformations are found, one derived from 6-s-trans with a twist angle of −166.3° and two from 6-s-cis, with −28.5 and 34.2° twist angles, respectively, and energies of 0.4 and 0.3 kcal/mol relative to the more stable 6-s-trans conformer. Hartree−Fock (HF) and DFT ab initio calculations have also shown that the planar 6-s-trans conformation of the free chromophore is energetically favored over the 6-s-cis conformation (*37*, *38*). In contrast to these theoretical results, the crystallographic data show a nonplanar 6-s-cis structure (*39*, *40*), possibly due to packing effect. The different twist angles of the two 6-s-cis conformers reflect the two possible conformations of the inverting cyclohexene ring. The signs of these angles are not relevant as long as the chromophore is considered in an achiral environment. For every twisted conformation, there exists a mirror-image structure, in which all dihedral angles have opposite signs. In the absence of chirally discriminating agents, these two structures have identical energies. This changes as the chromophore complexes with the chiral protein pocket which can discriminate between mirror-image conformations.

We have not calculated the complete potential energy curve of the torsional potential; however, it is known (*41*, *42*) that there is a rather high barrier separating the 6-s-cis and the 6-s-trans conformations; interconversion of the two *cis*-conformations is relatively easy. The SCC-DFTB calculated structures agree with ab initio calculations at the HF (*37*) and Density Functional levels of theory (*38*) and with an elaborate plane-wave expansion of the molecule (*43*).

Table 1: Summary of Calculation of the Rhodopsin Binding Pocket: Selected Dihedral Angles along Carbon Chain, Relative Energy and Twist of Most Stable Chromophore Conformations **1**−**5**

	C6C7	C9C10	C10C11	C11C12	C12C13	energy[a]	twist[b]
1	−34.7	176.2	174.7	−11.4	169.4	0.0	41.7
2	−157.6	173.9	175.1	−14.0	171.5	0.7	25.0
3	−148.2	175.7	175.6	−10.2	175.2	2.6	11.8
4	52.0	179.2	177.2	−8.0	169.1	3.6	11.9
5	127.3	176.1	173.9	−9.8	173.8	4.7	38.8

[a] Energy in kcal/mol relative to **1**. [b] Angle between C7−C10 and C15−N planes, experimental value 42° ± 10°.

Energy minimization of the rhodopsin protein pocket gives five stable conformations, each characterized by a peculiar conformation of the chromophore. Relative energies and selected dihedral angles along the unsaturated chain for all five conformers are given in Table 1. The existence of more local energy minima cannot be ruled out with certainty on a complicated potential energy surface like this. However, we have performed MD calculations on the two lowest-energy conformations and have found them rather robust with respect to small geometry variations. These two conformations, one representing a 6-s-cis, the other a 6-s-trans conformation, are shown in Figure 1a,b mapped against their respective planar precursors. They are separated by only 0.7 kcal/mol, and their stabilites are reversed relative to the isolated chromophore, i.e. in the protein environment the cis conformation becomes the most stable conformation. In both the 6-s-cis and the 6-s-trans conformations, the sign of the C6−C7 dihedral angle is negative. Starting with a 0° or a 180° dihedral angle, i.e., without any bias for sign of the resulting twist angle, the two conformations always come out with negative twist angle for this bond, indicating that there is strong chiral discrimination by the protein pocket for a negatively twisted β-ionone, be it the 6-s-cis or 6-s-trans arrangement.

The other major effect of the protein is the twist in the central part of the polyene chain, affecting mainly the three bonds from C10 to C13 and resulting in a kink of the chromophore. A measure of the overall twist is the angle formed by the approximate planes from C7 to C10 and from

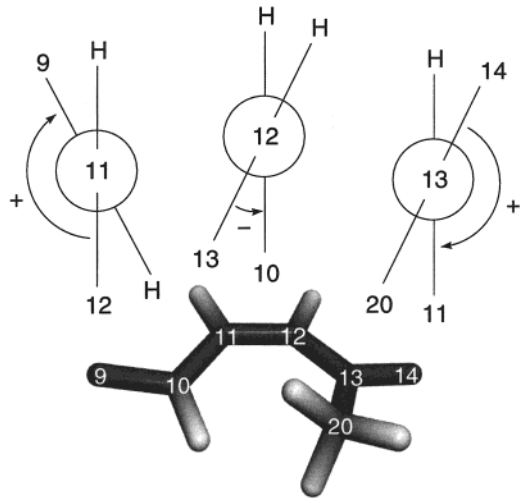

FIGURE 2: Close-up view of the helically distorted central part of the chromophore, from C9 to C14. Also shown are the Newman-projections of the three consecutive bonds, C10−C11, C11−C12, and C12−C13, to illustrate the convention used for the signs of the dihedral angles.

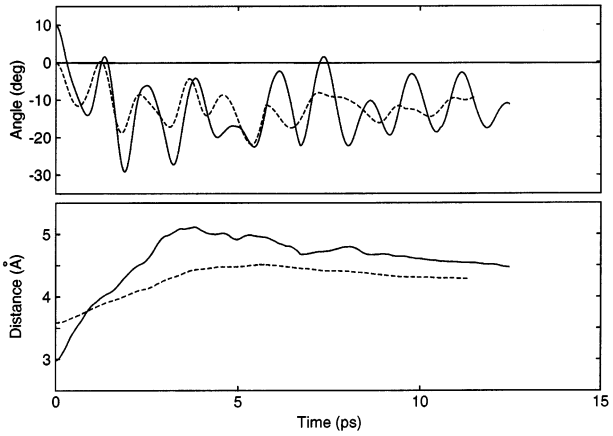

FIGURE 3: Time development of the C11−C12 dihedral angle (top) and the distance between the methyl groups of C13 and Ala117 for two starting geometries of the chromophore, one planar (solid line) and one with a + 10° dihedral angle of the C11−C12 bond (broken line).

C13 to C15. This angle ranges from 42° for the lowest-energy conformation to 12° for the less stable 6-s-cis conformation. The twist is concerted, i.e., the dihedral angles of the three consecutive bonds alternate in sign. Figure 2 shows in detail how these dihedral angles are defined. The distortion confers a helix-like geometry on this part of the chromophore; as a consequence the steric interaction between the C20 methyl group and the hydrogen at C10 is relieved. The sense of the helix is determined by the protein environment. Regardless of the starting geometry, the dihedral angle of the C11−C12 double bond always comes out to be negative and the C10−C11 and C12−C13 bonds positive. Figure 3 shows the results of two MD calculations where the development of the C11−C12 dihedral angle is plotted against time for two different starting geometries. In one, the chromophore geometry was taken to be planar from C11 to C13; in the other one, the simulation was started with a twist which was purposely chosen opposite to the one of the minimized structure, viz. +10° for the C11−C12 bond. From both starting geometries the chromophore rapidly moves into a helically twisted geometry, with the helix sense in agreement with what is calculated using the CG method. The net effect of the interaction is that the C20 methyl group is shifted toward the observer if the chromophore is oriented as in the Figure 2, i.e., the C12−C13 bond is twisted in a positive manner.

Also plotted in Figure 3 is the distance between the C20 methyl group and the methyl group of Ala117 which is the amino acid closest to this region of the chromophore. The starting distance of 3.6 Å (for the planar conformation of the chromophore) and 3.0 Å (for the chromophore with the opposite twist) rapidly increases, first over-shooting and then approximating the equilibrium distance of 4.2 Å.

How the chromophore conformation affects the protein environment is depicted in Figure 4, which presents an overlay of the two most stable pocket geometries with the chromophore in the 6-s-cis and the 6-s-trans geometry, respectively. Large movements of the amino acid residues are restricted to the region of the β-ionone ring (Phe212, Phe261, His211, and Trp265) and to rotation of the phenyl ring in Tyr268, close to C20. Note the relative rigidity of the protein environment close to C9 of the chromophore and its methyl group, which suggests a possible special interaction between this methyl group and the protein environmnent (*44*).

In addition to the nonplanar distortion, the chromophore suffers significant bond length changes as the result of binding to the protein. Figure 5 presents a plot of calculated bond lengths of the chromophore after equilibration in the protein pocket (●), together with the isolated SB both in the protonated (■) and in the deprotonated (▲) state. These latter data are added so that the effect of the protein pocket can be judged more clearly. The deprotonated SB shows strong bond alternation throughout the chromophore. As a result of protonation, bond alternation is significantly reduced in the vicinity of the positive center, from C15 to C9; beyond the two structures are rather similar. The protein-bound chromophore is intermediate between these two states, with strong bond alternation persisting throughout the conjugated chain.

DISCUSSION

There is abundant experimental evidence in support of the notion that the protein environment significantly affects the chromophore conformation and changes it from the solution (or vacuum) geometry. The relative energies of 11-*cis*- and all-*trans*-retinal are reversed upon binding to the protein; Resonance Raman, ^{13}C, and 2D NMR spectral analyses indicate that the chromophore is strongly twisted in the central part (*21*−*24*), and according to CD (circular dichroism) spectral data, there is even a preferred sense of twist of the chromophore (*45*, *46*). A wealth of experimental data has been accumulated concerning the "opsin shift", i.e., the UV−vis spectral shift which the chromophore undergoes as a consequence of protein binding and which is probably the combined result of structural and electronic changes of the chromophore (*47*−*50*). Do our calculations which represent the most rigorous treatment to date of the rhodopsin chromophore, including a relevant part of the protein environment, stand up against this evidence? In the following we discuss several of the pertinent questions.

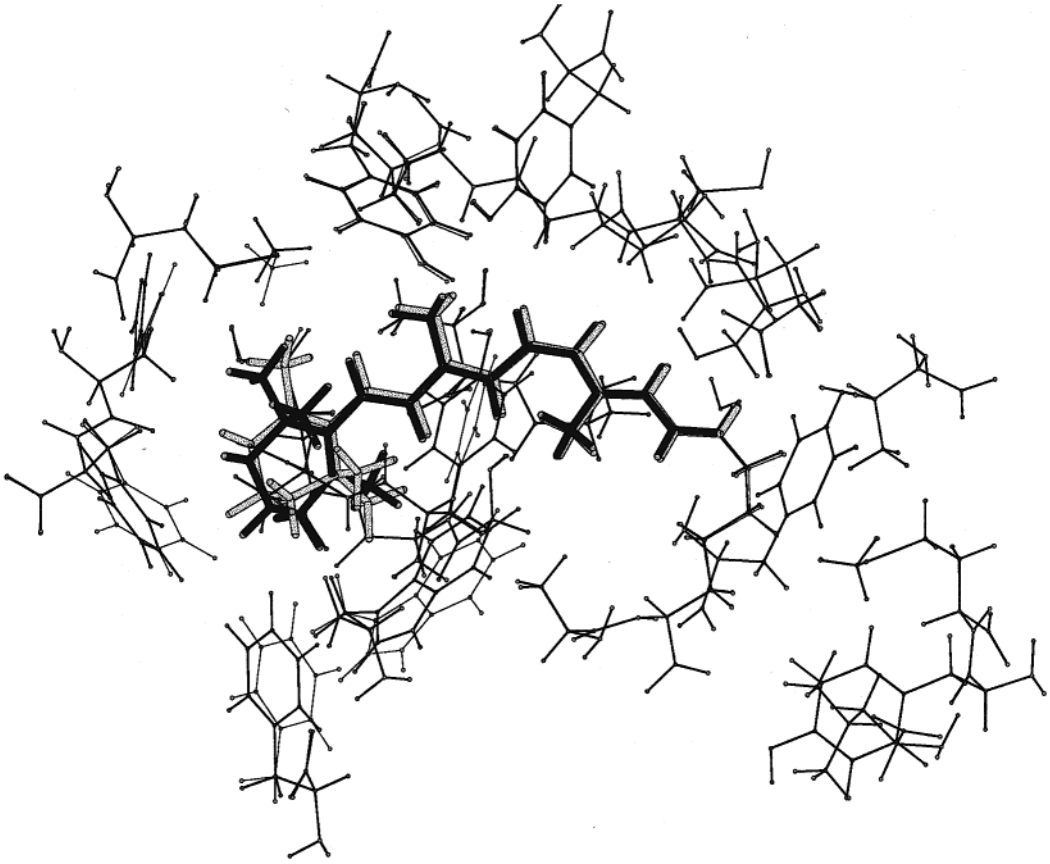

FIGURE 4: Overlay of the two minimum-energy structures of the protein pocket including the chromophores. Thin and thick lines correspond to the pocket adapted to the 6-s-cis and the 6-s-trans conformations, respectively.

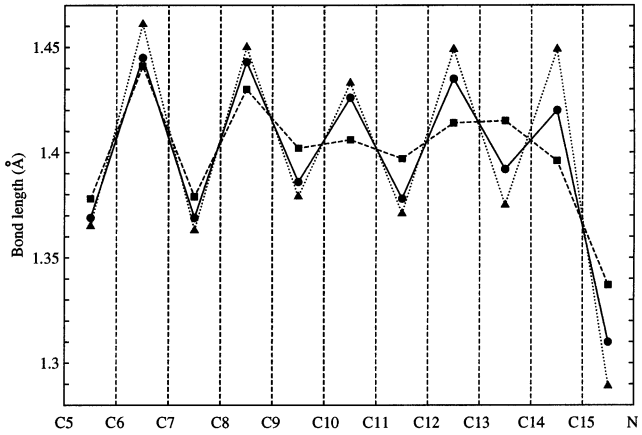

FIGURE 5: Bond lengths of the polyene chain of the chromophore optimized inside the protein pocket (●). Also shown are the bond lengths of the isolated 11-*cis*-retinal SB, both in the deprotonated (▲) and the protonated forms (■) optimized outside the pocket. The pattern of alternating short and long bonds which is lost in the SB as a result of protonation is partially recovered within the protein pocket.

The β-Ionone Ring Orientation. It has been a tenet in rhodopsin chemistry that the conformation of the β-ionone ring is 6-s-cis, and the X-ray diffraction data have been analyzed on this assumption. The study by Gröbner et al. (*19*) has thrown doubt on this assignment: preparing rhodopsin samples with chromophores in which each of the three methyl groups, at C5, C9, and C13, was substituted separately by CD_3, magic-angle-oriented sample spinning was applied to determine the angles of the three $C-CD_3$ bonds with respect to the external magnetic field. The values that were obtained were 21°, 44°, and 30°, each with a 5° error margin. Using distance constraints for the chromophore derived from other NMR-work (*22*), a model for the chromophore was deduced which allowed only two possible β-ionone conformations to fit the experimental data. Both are derived from 6-s-trans, one with a 152°, the other one with a 110° dihedral angle which is only 20° from perpendicular.

As a test whether our chromophore structures fit the requirements of the Gröbner experiment, we have oriented the two chromophores in space in such a manner as to achieve the best agreement with the experimentally determined orientation of the three bonds. Only the 6-s-trans geometry passes this test. Figure 6 shows the orientation of the chromophore; the resulting angles are 23°, 46°, and 30° with respect to the vertical axis, in perfect agreement with the NMR-data of Gröbner et al. We have found no possibility to orient either of the 6-s-cis conformations such that the bond orientations match the NMR data. Interestingly, the 6-s-trans structure which is inverted only at the C6−C7 bond, i.e., which has a dihedral angle of +157.6°, fits the model equally well, with orientation angles of 22°, 46°, and 30°. This structure is precluded, however, because it does not fit the protein pocket.

In several respects our conclusions match the ones reached by Birge et al. (*51*) who used an MNDO (modified neglect of diatomic overlap) type semiempirical model including singles and doubles CI (configuration iteration) to investigate the torsional potential around the C6−C7 bond of 11-*cis*-retinal pSb. For every torsional angle, the whole chromophore was geometry-optimized which included a carboxylate

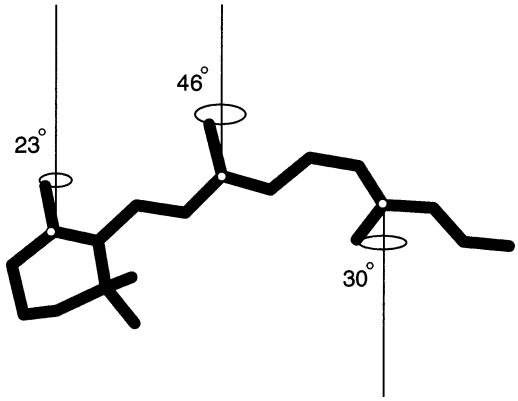

FIGURE 6: The minimum-energy structure of 6-s-*trans*,11-*cis*-retinal pSB in the protein pocket. The resulting angles are 23°, 46° and 30° with respect to the vertical axis, which are in perfect agreement with the NMR-data of Gröbner et al.

anion and a water molecule. The minimum near 140° for the β-ionone torsion angle which was found in that study is close to our result. Furthermore, the Birge model fits the Gröbner criteria and excludes, like ours, the 6-s-cis conformation of the chromophore. However, the twist of the chromophore chain which Birge found is completely different from ours (see below).

Evidence for the 6-s-cis assignment of the β-ionone ring in rhodopsin comes from solid-state NMR-spectral data of 11-*cis*-retinal labeled with ^{13}C at the C5 position. From a comparison of the principal tensor elements with ^{13}C5 labeled 6-s-cis and 6-s-trans retinoic acid, a nonplanar 6-s-cis conformation has been deduced for rhodopsin (*23*). Also, from binding studies of structurally locked retinal derivatives, the preference for the 6-s-cis conformation has been established (*52*). Our calculated energy difference of 0.7 kcal/mol between the two conformations is too small to support or disregard any of the two assignment. However, we note that the negative dihedral angle which we calculate for the stable 6-s-cis conformer agrees with the recent binding studies of two enantiomeric 6-s-cis locked retinoids by Nakanishi (*53*). A negative C6−C7 dihedral angle is also suggested on the basis of quantum-mechanical analysis of CD-spectral data of rhodopsin (*54*).

Nonplanar Deformation of the Chromophore. The nonplanar deformation of the chromophore by the protein environment has been suggested by a number of spectroscopic investigations. A quantitative measure has been provided by rotational resonance distance measurements on isotopically labeled rhodopsins yielding distances for the C10−C20 and the C11−C20 bonds of 3.0 and 2.9 Å, respectively, with error margins of ±0.015 Å (*22*). Molecular modeling of the chromophore on the basis of these distance constraints led to an estimated angle between the C7−C10 and the C13−C15 plane of the chromophore of ∼42° (*23*). The corresponding distances in our two minimum energy structures are 3.04/3.09 for the 6-s-trans conformer and 3.08/3.09 for the 6-s-cis conformer, in reasonable agreement with the experimental data. The calculated angle of 42° between the C7−C10 and C13−C15 planes in the 6-s-cis conformation versus only 25° for 6-s-trans is an argument in favor of the former. Another measure of the nonplanar deformation of the chromophore is the H−C10−C11−H torsional angle which deviates by 160 ± 10° from planar s-trans (*24*). Our calculated values of 164° (6-s-trans) and 166° (6-s-cis) are well within the quoted error margin.

Absolute Configuration of the Chromophore. The NMR spectroscopic data which have been discussed in the preceding paragraph cannot distinguish between oppositely twisted forms of the chromophore. The only spectroscopic method which is able to differentiate between quasi-enantiomeric conformations of the chromophore is CD, i.e., the difference in absorbance for left and right circular polarized light. From an analysis of the sign of the so-called α-band in the CD-spectrum of native rhodopsin at 480 nm, it was concluded that the torsion angle of the C12−C13 bond is positive (*54*, *55*), in agreement with the calculated structures of this study but in contrast to the prevailing notion (*56*−*59*). The conclusion that the torsion is positive has also been reached lately by Nakanishi et al. (*60*), who studied the protein binding of 11-*cis*-locked cyclopropyl retinals and found that only the diastereomer with a positive twist angle about the C12−C13 bond binds to opsin.

Bond Length Pattern. The retinal SB is definitely protonated in the protein pocket: our calculated distance between the proton and the SB nitrogen is 1.11 versus 1.55 Å to the counterion. However, with bond alternation visibly persisting throughout the conjugated chain, the rhodopsin chromophore resembles more the deprotonated than the protonated structure of the isolated SB (Figure 5). The reason for this apparent discrepancy is not to be found in the skeletal deformation of the chromophore: according to high-level CASPT2 (multi-configurational second-order perturbation theory) calculations (M. Schreiber and J. Hufen, unpublished results), out-of-plane torsion of any bond by up to 30° does not change bond lengths by more than 0.001 Å. Also, there are no charged groups in the vicinity of the chromophore except for the counterion which could localize the positive charge and increase bond alternation. The counterion, on the other hand, is known to significantly affect the electronic structure of the chromophore as evidenced, e.g., by ^{13}C chemical shifts along the polyene chain (*61*) or in the shift of absorption spectra (*49*). Our own calculations indicate that it is sufficient to weaken the N−H hydrogen bond by adding water as acceptor molecules for the proton. Just one water molecule significantly increases double-bond fixation, at the same time blue-shifting the absorption maximum by 18 nm.

CONCLUSION

We have studied the possible conformations of 11-*cis*-retinal pSB in a realistic binding pocket of rhodopsin consisting of 27 amino acids. With initial coordinates taken from X-ray diffraction data, we have followed how the protein affects the conformational space of the chromophore. We observe significant energy changes, with the protein stabilizing the 6-s-cis conformation relative to 6-s-trans, but not to the extent of excluding it. The protein induces a significant kink of the polyene chain as a result of concerted helical out-of-plane deformation of the chromophore chain. The protein pocket exerts strong chiral discrimination: the negatively twisted 6-s-cis conformation is almost 4 kcal/mol more stable than the pseudo-enantiomer with a positive twist angle. The positively twisted 6-s-trans conformation is not stable, and neither is the conformation with a negative C12−C13 dihedral angle.

We assume that the chromophore geometries derived at in this study present a reliable basis for more elaborate efforts concerning the structure and dynamics of the ground state and of subsequent intermediates.

NOTE

After completion of this manuscript, two studies about the relative orientation of the β-ionone ring were published. Spooner et al. (*62*) concluded on the basis of rotational resonance solid-state NMR measurements of selectively ^{13}C-labeled retinals that the binding pocket is populated by two conformational states, a minor component comprising about 26% and corresponding possibly to a twisted 6-s-trans form, and a major component which the authors identify as the 6-s-cis conformer. These data comply with the results of our study. A 0.7 kcal/mol energy difference translates into a 3:1 equilibrium population at room temperature. Also, the experimentally determined structural data of the more stable 6-s-cis conformer agree remarkably well with our data: dihedral angle C5−C6−C7−C8, $-28 \pm 7°$ (our value: $-35°$); C8−C5 methyl, 2.95 ± 0.15 Å (2.994 Å); C8−C1 methyls, 4.05 ± 0.25 Å (4.342/3.981 Å). On the other hand, Creemers et al. (*63*) report the results of magic angle spinning NMR spectroscopy using ^{13}C labeled retinals. Their data do not show additional signals which have been observed by Spooner et al. They conclude that the additional signals can be explained as impurities due to retinal derivatives and that therefore the β-ionone ring conformation is unique.

REFERENCES

1. Hubbard, R. (1969) Absorption spectrum of rhodopsin: 500 nm absorption band, *Nature 221*, 432−435.
2. Yoshizawa, T., and Wald, G. (1963) Pre-lumirhodopsin and the bleaching of visual pigments, *Nature 197*, 1279−1286.
3. Wald, G. (1968) Molecular basis of visual excitation, S*cience 162*, 230−239.
4. Schoenlein, R. W., Peteanu, L. A., Mathies, R. A., and Shank, C. V. (1991) The first step in vision: femtosecond isomerization of rhodopsin, *Science 254*, 412−415.
5. DeLange, F., Bovee-Geurts, P. H. M., VanOostrum, J., Portier, M. D., Verdegem, P. J. E., Lugtenburg, J., and DeGrip, W. J. (1999) An additional methyl group at the 10-position of retinal drastically slows down the kinetics of the rhodopsin photocascade, *Biochemistry 37*, 1411−1420.
6. Palings, I., Pardoen, J. A., van den Berg, E., Winkel, C., Lugtenburg, J., and Mathies, R. A. (1987) Assignment of fingerprint vibrations in the resonance Raman spectra of rhodopsin, isorhodopsin, and bathorhodopsin: implications for chromophore structure and environment, *Biochemistry 26*, 2544−2556.
7. Jäger, S., Lewis, J. W., Zvyaga, T. A., Szundi, I., Sakmar, T. P., and Kliger, D. S. (1997) Time-resolved spectroscopy of the early photolysis intermediates of rhodopsin Schiff base counterion mutants, *Biochemistry 36*, 1999−2009.
8. Jäger, F., Ujj, L., and Atkinson, G. H. (1997) Vibrational spectrum of bathorhodopsin in the room-temperature rhodopsin photoreaction, *J. Am. Chem. Soc. 119*, 12610−12618.
9. Borhan, B., Souto, M. L., Imai, H., Shichda, Y., and Nakanishi, K. (2000) Movement of retinal along the visual transduction path, *Science 288*, 2209−2212.
10. Kim, J. E., McCamant, D. W., Zhu, L., and Mathies, R. A. (2001) Resonance Raman structural evidence that the cis-to-trans isomerization in rhodopsin occurs in femtoseconds, *J. Phys. Chem. B 105*, 1240−1249.
11. Doukas, A. G., Aton, B., Callender, R. H., and Ebrey, T. G. (1978) Resonance Raman studies of bovine metarhodopsin I and metarhodopsin II, *Biochemistry 12*, 2430−2435.
12. Jäger, F., Jäger, S., Kräutle, O., Friedman, N., Sheves, M., Hofmann, K. P., and Siebert, F. (1994) Interactions of the β-ionone ring with the protein in the visual pigment rhodopsin control the activation mechanism. An FTIP and fluorescence study on artificial vertebrate rhodopsins, *Biochemistry 33*, 7389−7397.
13. Gorczyca, W. A., Gray-Keller, M. P., Detwiler, P. B., and Palczewski, K. (1994) Purification and physiological evaluation of a guanylate cyclase activating protein from retinal rods, *Proc. Natl. Acad. Sci. U.S.A. 91*, 4014−4018.
14. Palczewski, K., Kumasaka, T., Hori, T., Behnke, C. A., Motoshima, H., Fox, B. A., LeTrong, I., Teller, D. C., Okada, T., Stenkamp, R. E., Yamamoto, M., and Miyano, M. (2000) Crystal structure of rhodopsin: a G protein-coupled receptor, *Science 289*, 739−745.
15. Teller, D. C., Okada, T., Behnke, C. A., Palczewki, K., and Stenkamp, R. E. (2001) Advances in determination of a high-resolution three-dimensional structure of rhodopsin, a model of G-protein-coupled receptors (GPCRs), *Biochemistry 40*, 7761−7772.
16. Zhukovski, E. A., and Oprian, D. D. (1989) Effect of carboxylic acid side chains on the absorption maximum of visual pigments, *Science 246*, 928−930.
17. Nathans, J. (1990) Determinants of visual pigment absorbance: identification of the retinylidene Schiff's base counterion in bovine rhodopsin, *Biochemistry 29*, 9746−9752.
18. Han, M., and Smith, S. O. (1995) NMR constraints of the location of the retinal chromophore in rhodopsin and bathorhodopsin, *Biochemistry 34*, 1425−1432.
19. Gröbner, G., Burnett, I. J., Glaubitz, C., Choi, G., Mason, A. J., and Watts, A. (2000) Observations of light-induced structural changes of retinal within rhodopsin, *Nature 405*, 810−813.
20. Nakanishi, K. (2000) Recent bioorganic studies on rhodopsin and visual transduction, *Chem. Pharm. Bull. 48*, 1399−1409.
21. Lin, S. W., Groesbeek, M., van der Hoef, I., Verdegem, P., Lugtenburg, J., and Mathies, R. A. (1998) Vibrational assignment of torsional normal modes of rhodopsin: probing excited-state isomerization dynamics along the reactive C_{11}═C_{12} torsion coordinate, *J. Phys. Chem. B 102*, 2787−2806.
22. Verdegem, P. J. E., Bovee-Geurts, P. H. M., de Grip, W. J., Lugtenburg, J., and DeGroot, H. J. M. (1999) Retinylidene ligand structure in bovine rhodopsin, metarhodopisn-I, and 10-methyl-rhodopsin from internuclear distance measurements using ^{13}C-labeling and 1-D rotational resonance MAS NMR, *Biochemistry 38*, 11316−11324.
23. Mathies, R. A., and Lugtenburg, J. (2000) The primary photoreaction of rhodopsin, in *Handbook of Biological Physics* (Stavenga, D. G., DeGrip, W. J., and Pugh, E. N., Jr., Eds.) Vol. 3, Chapter 2, pp 55−90, North-Holland, Amsterdam.
24. Feng, X., Verdegem, P. J. E., Lee, Y. K., Sandström, D., Edén, M., Bonvee-Geurts, P., DeGrip, W. J., Lugtenburg, J., de Groot, H. J. M., and Levitt, M. H. (1997) Direct determination of a molecular torsional angle in the membrane protein rhodopsin by solid-state NMR, *J. Am. Chem. Soc. 119*, 6853−6857.
25. Warshel, A., and Barboy, N. (1982) Energy storage and reaction pathways in the first step of the vision process, *J. Am. Chem. Soc. 104*, 1469−1476.
26. Wang, Q., Schoenlein, R. W., Peteanu, L. A., Mathies, R. A., and Shank, C. V. (1994) Vibrationally coherent photochemistry in the femtosecond primary event of vision, *Science 266*, 422−424.
27. Garavelli, M., Bernardi, F., Olivucci, M., Vreven, T., Klein, S., Celani, P., and Robb, M. A. (1998) Potential-energy surfaces for ultrafast photochemistry static and dynamics aspects, *Faraday Discuss. 110*, 51−70.
28. Elstner, M., Porezag, D., Jungnickel, G., Elsner, J., Haugk, M., Frauenheim, T., Suhai, S., and Seifert, G. (1998) Self-consistent-charge density-functional tight-binding method for simulations of complex materials properties, *Phys. Rev. B 58*, 7260−7268.
29. Frauenheim, T., Seifert, G., Elstner, M., Hajnal, Z., Jungnickel, G., Porezag, D., Suhai, S., and Scholz, R. (2000) A self-consistent charge density-functional based tight-binding method for predictive materials simulations in physics, chemistry, biology, *Phys. Stat. Sol. (b) 217*, 41−62.
30. Elstner, M., Frauenheim, T., Kaxiras, E., Seifert, G., and Suhai, S. (2000) A self-consistent charge density-functional based tight-binding scheme for large biomolecules, *Phys. Status Solidi B 217*, 357−376.
31. Zhou, H., Tajkhorshid, E., Frauenheim, T., Suhai, S., and Elstner, M., (2002) Performance of the AM1, PM3, and SCC-DFTB methods in the study of conjugated Schiff base molecules, *Chem. Phys. 277*, 91−103.

32. Fahmy, K., Jäger, F., Beck, M., Zvyaga, T. A., Sakmar, T. P., and Siebert, F. (1993) Protonation states of membrane-embedded carboxylic acid groups in rhodopsin and metarhodopsin II: a Fourier-transform infrared spectroscopy study of site-directed mutans, *Proc. Natl. Acad. Sci. U.S.A. 90*, 10206−10210.
33. Yan, E. C. Y., Kazmi, M. A., De, S., Chang, B. S. W., Seibert, C., Marin, E. P., Mathies, R. A., and Sakmar T. P. (2002) Function of extracellular loop 2 in rhodopsin: glutamic acid 181 modulates stability and absorption wavelength of metarhodopsin II, *Biochemisty 41*, 3620−2627.
34. Birge, R. R., Murray, L. R., Peierce, B. M., Akita, H., Balogh-Nair, V., Findsen, L. A., and Nakanishi, K. (1985) Two-photon spectroscopy of locked-11-cis-rhodopsin: evidence for a protonated Schiff base in a neutral protein binding site, *Proc. Natl. Acad. Sci. U.S.A. 82*, 4117−4121.
35. Nagata, T., Terakita, A., Kandori, H., Kojima, D., Schichida, Y., and Maeda, A. (1997) Water and peptide backbone structure in the active center of bovine rhodopisn, *Biochemistry 36*, 6164−6170.
36. Nagata, T., Terakita, A., Kandori, H., Schichida, Y., and Maeda, A. (1998) The hydrogen-bonding network of water molecules and the peptide backbone in the region connecting Asp83, Gly120, and Glu113 in bovine rhodopsin, *Biochemistry 37*, 17216−17222.
37. Terstegen, F., and Buss, V. (1996) All-trans and 11-cis-retinal, their N-methyl Schiff base and N-methyl protonated Schiff base derivatives: a comparative ab initio study, *J. Mol. Struct. (THEOCHEM) 369*, 53−65.
38. Terstegen, F., and Buss, V. (1998) Influence of DFT-calculated electron correlation on energies and geometries of retinals and of reinal derivatives related to the bacteriorhodopsin and rhodopsin chromophores, *J. Mol. Struct. (THEOCHEM) 430*, 209−218.
39. Stam, C. H., and MacGillavry, C. H. (1963) The crystal structure of the triclinic modification of vitamin-A acid, *Acta Crystallogr. 16*, 62−68.
40. Stam, C. H. (1972) The crystal structure of a monoclinic modification and the refinement of a triclinic modification of vitamin A acid (retinoic acid), $C_{20}H_{28}O_2$, *Acta Crystallogr., Sect. B 28*, 2936−2945.
41. Terstegen, F., and Buss, V. (1996) Ab initio study of the C6−C7 conformation of retinal model systems, *Chem. Lett.* 449−450.
42. Terstegen, F., Carter, E. A., and Buss, V. (1999) Interconversion pathways of the protonated β-ionone Schiff base: an ab initio molecular dynamics study, *Intern. J. Quantum Chem. 75*, 141−145.
43. Sugihara, M., Entel, P., Meyer, H., Buss, V., Terstegen, F., and Hafner, J. (2000) A molecular-dynamics study of the rhodopsin chromophore using ultrasoft pseudopotentials, *Prog. Theor. Phys. Suppl. 138*, 107−112.
44. Han, M., Groesbeek, M., Sakmar, T. P., and Smith, S. O. (1997) The C9 methyl group of retinal interacts with glycine-121 in rhodopisn, *Proc. Natl. Acad. Sci. U.S.A. 94*, 13442−13447.
45. Fukuda, Y., Shichida, Y., Yohizawa, T., Ito, M., Kodama, A., and Tsukida, K. (1984) Studies on structure and functions of rhodopsin by use of cyclopentarienylidene 11-cis-locked-rhodopsin, *Biochemistry 23*, 5826−5832.
46. Ito, M., Katuta, Y., Imamoto, Y., Shichida, Y., and Yoshizawa, T. (1992) Conformational analysis of the rhodopsin chromophore using bicyclic retinal anlaogues, *Photochem. Photobiol. 56*, 915−919.
47. Honig, B., Dinur, U., Nakanishi, K., Balogh-Nair, V., Gawinowicz, M. A., Arnaboldi, M., and Motto, M. G. (1979) An external potincharge model for wavelengh regulation in visual pigments, *J. Am. Chem. Soc. 101*, 7084−7086.
48. Kakitani, H., Kakitani, T., Rodman, H., and Honig, B. (1985) On the mechanism of wavelength regulation in visual pigment, *Photochem. Photobiol. 41*, 471−479.
49. Hu, J., Griffin, R. G., and Herzfeld, J. (1994) Synergy in the spectral tuning of retinal pigments: complete accounting of the opsin shift in bacteriorhodopsin, *Proc. Natl. Acad. Sci. U.S.A. 91*, 8880−8884.
50. Nathans, J. (1999) The evolution and physiology of human color vision: insight from molecular genetic studies of visual pigments, *Neuron 24*, 299−312.
51. Singh D., Hudson, B. S., Middleton C., and Birge, R. R. (2001) Conformation and orientation of the retinyl chromophore in rhodopsin: a critical evaluation of recent NMR data on the basis of theoretical calculations results in a minimum energy structure consistent with all experimental data, *Biochemistry 40*, 4201−4204.
52. Imamoto, Y., Sakai, M., Katuta, Y., Wada, A., Ito, M., and Shichida., Y. (1996) Structure around C_6-C_7 bond of the chromophore in bathorhodopsin: low-temperature spectrosocopy of 6-s-cis-locked bicyclic rhodopsin analogues, *Biochemistry 35*, 6257−6262.
53. Fujimoto, Y., Ishihara, J., Maki, S., Fujioka, N., Wang, T., Furuta, T., Fishkin, N., Borhan, B., Berova, N., and Nakanishi, K. (2001) On the bioactive conformation of the rhodopsin chromophore: absolute sense of twist around the 6-s-cis bond, *Chem. Eur. J. 7*, 4198−4204.
54. Buss, V. (2001) Inherent chirality of the retinal chromophore in rhodopsin − a nonempirical theoretical anlysis of chiroptical data, *Chirality 13*, 13−23.
55. Buss, V., Kolster, K., Terstegen, F., and Vahrenhorst, R. (1998) Absolute sense of twist of the C12−C13 bond of the retinal chromophore in rhodopsin − semiempirical and nonempirical calculations of chiroptical data, *Angew. Chem., Int. Ed. Engl. 37*, 1893−1895.
56. Kakitani, H., Kakitani, S., and Yomosa, S. (1977) Molecular mechanism for the initial process of visual excitation. II. Theoretical analysis of optical activity in rhodopsin and bathorhodopsin, *J. Phys. Soc. Jpn. 42*, 996−1004.
57. Han, M., and Smith, S. O. (1997) Corrections, *Biochemistry 36*, 7280.
58. Tan, Q., Lou, J., Borhan, B., Karnaukhova, E., Berova, N., and Nakanishi, K. (1997) Absolute sense of twist of the C12−C13 bond of the retinal chromophore in bovine rhodopsin based on exciton-coupled CD spectra 11,12-dihydroretinal analogues, *Angew. Chem., Int. Ed. Engl. 36*, 2089−2093.
59. Lou, J., Hashimoto, M., Berova, N., and Nakanishi, K. (1999) Enantioselective binding of an 11-cis-locked cyclopropyl retinal. The conformation of retinal in bovine rhodopsin, *Org. Lett. 1*, 51−54.
60. Fujimoto, Y., Fishkin, N., Pescitelli, G., Decatur, J., Berova, N., and Nakanishi, K. (2002) Solution and biologically relevant conformations of enantiomeric 11-cis-locked cyclopropyl retinals, *J. Am. Chem. Soc. 124*, 7294−7302.
61. Sakurai, M., Wada, M., Inoue, Y., Tamura, Y., and Watanabe, Y. (1996) Ab initio study of ^{13}C NMR chemical shifts for the chromophores of rhodopsin and bacteriorhodopsin. 2. Comprehensive analysis of the ^{13}C chemical shifts of protonated all-trans-retinylidene Schiff base, *J. Phys. Chem. 100*, 1957−1964.
62. Spooner, P. J. R., Sharples, J. M., Verhoeven, M. A., Lugtenburg, J., Glaubitz, C., and Watts, A. (2002) Relative orientation between the β-ionone ring and the polyene chain for the chromophore of rhodopsin in native membranes, *Biochemistry 41*, 7549−7555.
63. Creemers, A. F. L., Kiihne, S., Bovee-Geurts, P. H. M., DeGrip, W. J., Lugtenburg, J., and de Groot, H. J. M. (2002) ^1H and ^{13}C MAS NMR evidence for pronounced ligand-protein interactions involving the ionone ring of the retinylidene chromophore in rhodopsin, *Proc. Natl. Acad. Sci. U.S.A. 99*, 9101−9106.

BI020533F